DOI 10.1007/s10891-022-02632-6
Journal of Engineering Physics and Thermophysics, Vol. 95, No. 7, November, 2022

A COMPARATIVE ANALYSIS OF TWO APPROACHES TO NONLOCAL DUCTILE DAMAGE MODELING

V. S. Klyuchantsev and A. V. Shutov UDC 539.37

A new nonlocal version of Gurson–Tvergaard–Needleman model is presented, which includes a new scheme of delocalization of constitutive relations. The delocalization scheme has the effect of trapping the damage, which makes it possible to increase the accuracy of modeling the processes of destruction and to avoid excessive diffusion of material damage. As an alternative approach, a nonlocal thermodynamically consistent model of damage accumulation developed earlier is considered. For both models, efficient schemes of integrating constitutive relations are presented. Using the problem of the destruction of a strip with a hole as an example, the results obtained by both models are compared. Despite the fact that the models under consideration are based on fundamentally different hypotheses, the predicted integral characteristics and distributions of plastic strains coincide with high accuracy. The coincidence of the predictions by two different models greatly complicates the choice of model hypotheses based on integral characteristics. It is established, however, that for the two models there is a significant discrepancy in the predictions of the local evolution of the porosity of the material. Thus, in the presence of reliable experimental data on local material damage, this effect can be used as the basis for new protocols for selecting and calibrating models.

Keywords: *nonlocal damage mechanics, large deformations, Gurson–Tvergaard–Needleman model, finite element method.*

Introduction. Accumulation of damage and fracture of metallic structures in the regime of plastic deformations is the dominant factor that limits the strength of a wide range of technical products. The most accurate modeling of damage accumulation and strain localization is necessary for the rational application of the strength reserves of structural alloys used. In the present work, damage accumulation in a material is modeled using continuum damage mechanics, the foundations of which were laid by L. M. Kachanov [1, 2]. Within the framework of this continuum approach, internal variables are introduced that describe the degree of damage of the material for each material particle, and the corresponding evolution equations are postulated.

It is known that when performing calculations by the finite element method, the strain-softening behavior leads to a pathological mesh sensitivity of the finite element solution [3, 4]. Namely, when the mesh is refined, the deformation tends to be localized on the null set, which, in turn, leads to an underestimation of the crack resistance of the material. Similar problems with the pathological dependence of the numerical solution on discretization are also observed when working with meshless methods. Thus, within the smoothed particle hydrodynamics the fracture toughness of the material tends to zero on a decrease in the spatial discretization parameter [4, 5]. A pragmatic approach to solving this problem is to work only with finite elements of certain size [6]. In this case, the fixed size of the element becomes an additional parameter of the material [7]. The disadvantage of this technique is the impossibility of mesh refinement, as well as the significant dependence of the solution on the chosen discretization method. A scientifically based method for solving the problem of pathological dependence is to introduce nonlocal constitutive relations [3]. In the case of nonlocal modeling, stresses at a considered point in space depend on the strain history not only at this point, but also on strains in a certain neighborhood. In this work, we apply the so-called integral-based approach to the construction of nonlocal relations, which is based on the integral averaging operator. The averaging operator contains at least one scalar parameter, which is often identified with the characteristic size of the microstructure. It is the presence of a characteristic linear parameter in the model that limits the

M. A. Lavrent′ev Institute of Hydrodynamics, Siberian Branch of the Russian Academy of Sciences, 15 Acad. Lavrent′ev Ave., Novosibirsk, 630090, Russia; Novosibirsk State University, 1 Pirogov Str., Novosibirsk, 630090, Russia; email: alexey.v.shutov@gmail.com. Translated from Inzhenerno-Fizicheskii Zhurnal, Vol. 95, No. 7, pp. 1680–1692, November–December, 2022. Original article submitted December 9, 2021.

localization of deformations and makes it possible to obtain physically meaningful solutions [3, 4, 8, 9]. The choice in favor of the integral-based approach was made because of its suitability for embedding information about the microstructure of the material, in particular, about the presence of pronounced anisotropy [4]. In this case, the needed detailed information about the evolution of the microstructure can be obtained by the methods of high-resolution x-ray tomography [10–13].

In the field of plastic metal forming, as well as in simulating emergency scenarios, the most popular is the Gurson–Tvergaard–Needleman (GTN) model [14, 15]. In the present article, its nonlocal analogue is presented. The large strain kinematics is described using a set of multiplicative decompositions of the deformation gradient tensor. As shown in [16], working with multiplicative decompositions has a number of advantages over alternative methods of geometrically nonlinear description of the kinematics of inelastic strain. As an alternative to the Gurson–Tvergaard–Needleman model, the thermodynamically consistent (TDC) model proposed earlier in [4] is also considered. The thermodynamically consistent model is also based on multiplicative decompositions and on the integral approach to delocalization, but it contains a number of fundamentally different hypotheses.

Continuum Description of Damage and Fracture of Material. *Thermodynamically consistent model on the reference configuration.* Within the continuum damage mechanics the damage is taken to mean the appearance, growth, and integration of microscopic defects in a material. Work [4] presents a nonlocal thermodynamically consistent model, which is a generalization of the model described in [17]. To take into account the increase in the porosity of the material caused by plastic strain we divide the deformation gradient tensor $\mathbf{F}$ into an elasto-plastic part $\mathbf{F}_{ep}^{por}$ and volume expansion $\mathbf{F}_{por}$. According to the classical work of Bammann and Aifantis, the part $\mathbf{F}_{ep}^{por}$ is considered to be purely volumetric. A change in the volume associated with porosity is equal to $\Phi_{por} \geq 1$. Thus,

$$\mathbf{F} = \mathbf{F}_{ep}^{por}\mathbf{F}_{por}\ , \quad \mathbf{F}_{por} = \Phi_{por}^{1/3}1\ , \quad \det \mathbf{F}_{por} = \Phi_{por}\ . \tag{1}$$

Next, we use the classical multiplicative decomposition of the elasto-plastic part into an inelastic part $\mathbf{F}_{i}^{por}$ and elastic part $\mathbf{F}_{e}$:

$$\mathbf{F}_{ep}^{por} := \mathbf{F}_{e}\mathbf{F}_{i}^{por}\ , \quad \mathbf{C}_{i} := \mathbf{F}_{i}^{por,T}\mathbf{F}_{i}^{por}\ , \quad \mathbf{C} := \mathbf{F}^{T}\mathbf{F}\ . \tag{2}$$

For the simplicity of presentation, the equations of the model will be written on the reference configuration. The local state of the material is described by internal variables, such as the inelastic right Cauchy–Green tensor $\mathbf{C}_i$, accumulated plastic arc length s, and the porosity of the material Φ. The limiting cases $\Phi = 1$ and $\Phi \to \infty$ correspond to an intact state and to a completely destroyed state, respectively. The right Cauchy–Green tensor $\mathbf{C} = \mathbf{F}^T\mathbf{F}$ and its inelastic counterpart $\mathbf{C}_i$ are symmetric and positive definite. Inelastic flow is incompressible: $\det(\mathbf{C}_i) = 1$. The relationships between stresses and elastic strains are assigned by the law of hyperelasticity [18]. Following Richter [19], we assume that the Helmholtz free energy function is additively decomposed into volumetric and isochoric parts. Let us assume that the isochoric part corresponds to the neo-Hookean material, and the volumetric part is described by the Hartmann–Neff hypothesis [20]:

$$\tilde{\mathbf{T}} = \frac{k(\Phi)}{10}\left((\sqrt{\det \mathbf{C}}/\Phi)^5 - (\sqrt{\det \mathbf{C}}/\Phi)^{-5}\mathbf{C}^{-1}\right) + \mu(\Phi)\mathbf{C}^{-1}(\bar{\mathbf{C}}\mathbf{C}_i^{-1})^D. \tag{3}$$

Here $\tilde{\mathbf{T}}$ is the second Piola–Kirchhoff tensor, $k(\Phi)$ and $\mu(\Phi)$ are the bulk and shear moduli depending on porosity, $\bar{\mathbf{A}} = (\det \mathbf{A})^{-1/3}\mathbf{A}$ is the unimodular part of the tensor, $\mathbf{A}^D = \mathbf{A} - \frac{1}{3}\operatorname{tr}(\mathbf{A})\mathbf{1}$ is the deviatoric part of the tensor. The norm of the driving force of plastic flow is equal to

$$\mathfrak{F} = \Phi^{-1}\sqrt{\operatorname{tr}\left[(\mathbf{C}\tilde{\mathbf{T}})^D\right]^2}\ . \tag{4}$$

Inelastic (plastic) flow is described by equation [4]

$$\frac{\mathrm{d}}{\mathrm{d}t}\mathbf{C}_i = 2\frac{\lambda_i}{\mathfrak{F}}\Phi^{-1}(\mathbf{C}\tilde{\mathbf{T}})^D\mathbf{C}_i\ . \tag{5}$$

With account taken of formula (3), the plastic flow rule is written in a simplified form as

$$\frac{\mathrm{d}}{\mathrm{d}t}\,\mathbf{C}_\mathrm{i} \;=\; 2\,\frac{\lambda_\mathrm{i}}{\mathfrak{F}}\;\Phi^{-1}\mu(\Phi)(\bar{\mathbf{C}}\mathbf{C}_\mathrm{i}^{-1})^{D}\mathbf{C}_\mathrm{i}\;. \tag{6}$$

The scalar intensity of plastic flow is calculated in accordance with the viscoplasticity law:

$$\lambda_\mathrm{i} \;=\; \frac{1}{\eta}\left\langle\frac{f_\mathrm{overstress}}{f_0}\right\rangle^{m}\;,\quad f_\mathrm{overstress} \;=\; \mathfrak{F} - \sqrt{\frac{2}{3}}\,[K(\Phi) + R(s,\,\Phi)]\;. \tag{7}$$

Here, η and m are the material constants, $K(\Phi)$ is the yield stress dependent on the actual porosity, $R(s, \Phi)$ is the isotropic hardening, $\langle x\rangle = \max(0, x)$ is the positive part of the number x, $f_0 = 1$ MPa is the unit of stress used to obtain a non-dimensional expression in the angle brackets. The plastic arc length s controls the Voce isotropic hardening:

$$\dot{s} \;=\; \sqrt{\frac{2}{3}}\lambda_\mathrm{i}\;,\quad R(s,\,\Phi) \;=\; \Phi^{-1}\;\frac{\gamma(\Phi)}{\beta}\,(1 - \exp\,(1 - \beta s))\;, \tag{8}$$

where $\gamma(\Phi)$ is the material function and $\beta > 0$ is the fixed parameter of the material.

It is often assumed in the damage mechanics that all components of the elasticity tensor decrease synchronously [21]. However, in this work, calculations are performed taking into account that the rates of deterioration in individual strength characteristics of the material with damage accumulation are different [4]:

$$k(\Phi) \;=\; k_0\;\exp\,(-\mathrm{BRR}(\Phi - 1))\;,\quad \mu(\Phi) \;=\; \mu_0\;\exp\,(-\mathrm{SRR}(\Phi - 1))\;, \tag{9}$$

$$\gamma(\Phi) \;=\; \gamma_0\;\exp\,(-\mathrm{IRR}(\Phi - 1))\;,\quad K(\Phi) \;=\; K_0\Phi^{-1}\;\exp\,(-\mathrm{IRR}(\Phi - 1))\;, \tag{10}$$

where BRR, SRR, and IRR are material constants that determine the rates of deterioration of its strength characteristics; k_0, μ_0, γ_0, and K_0 are the constants that determine the characteristics of an undamaged material.

Within the local model, the increase in the porosity Φ of the material occurs as a result of the nucleation of new pores and the growth of the already existing ones:

$$\dot{\Phi}^{\mathrm{local}} \;=\; A_\mathrm{nucl}\lambda_\mathrm{i} + d_\mathrm{growth}\;\;(\Phi - \Phi_0)\lambda_\mathrm{i}\;\exp\left(\sqrt{\frac{3}{2}}\;\frac{\mathrm{tr}\;(\mathbf{C}\tilde{\mathbf{T}})}{\sqrt{\mathrm{tr}\;[(\mathbf{C}\tilde{\mathbf{T}})^{D}]^2}}\right), \tag{11}$$

where $A_\mathrm{nucl} \geq 0$, $d_\mathrm{growth} \geq 0$, and Φ_0 are the constants of the material. Note that the growth of the existing pores depends on the stress triaxiality. The system of constitutive relations is closed by specifying the initial conditions and by the delocalization procedure.

While using nonlocal models for the modeling of fracture, excessive diffusion of damage is often observed. Works [22, 23] are devoted to the solution of this problem with the aid of ad hoc hypotheses. Following work [4], to reduce the unrealistic diffusion in the model the damage trapping effect is applied. For this, an additional parameter of continuity Ψ is introduced. The continuity and porosity of the material are dual:

$$\Psi \;=\; \exp\,(-\mathrm{PCR}\;(\Phi - 1))\;,\quad \Phi \;=\; 1 - \log\,(\Psi)/\mathrm{PCR}\;, \tag{12}$$

where $\mathrm{PCR} > 0$ is the parameter of the material that specifies the ratio between the porosity and continuity. To produce the desired damage trapping effect, the material model is delocalized by applying an averaging operator to the continuity rate $\dot{\Psi}$ [4].

In this work, attention is mainly paid to nonlocal damage models of integral type. Let Body be the global configuration of the body under consideration. Depending on the delocalization procedure, Body can correspond to the global reference or global current configurations [8, 4]. Having a field of local values $q^{\mathrm{local}}(\mathbf{x})$, $\mathbf{x} \in$ Body, its nonlocal counterpart is obtained using the delocalization operation, also known as spatial averaging [24]:

$$q^{\mathrm{nl}}(\mathbf{x}) \;=\; (q^{\mathrm{local}})^{\mathrm{deloc}}(\mathbf{x}) \;=\; \int\limits_{\mathrm{Body}} q^{\mathrm{local}}(\mathbf{y})\,\alpha_\mathrm{deloc}(\mathbf{x},\,\mathbf{y})\;\mathrm{d}\mathbf{y}\;,\quad \mathbf{x} \in \mathrm{Body}\;, \tag{13}$$

where α_{deloc} is the delocalization kernel. According to (13), the local value in the source $\mathbf{y} \in$ Body goes over into the receiver $\mathbf{x} \in$ Body with the weight $\alpha_{\text{deloc}}(\mathbf{x}, \mathbf{y})$. In order that any nonlocal quantity could surely coincide with its local counterpart for any homogeneous process, the kernel must satisfy the normalization condition:

$$\int\limits_{\text{Body}} \alpha_{\text{deloc}}(\mathbf{x}, \mathbf{y})\, d\mathbf{y} = 1\,, \quad \mathbf{x} \in \text{Body}\,. \tag{14}$$

In this work, we use the delocalization kernel

$$\alpha_{\text{deloc}}(\mathbf{x}, \mathbf{y}) = \frac{\alpha_\infty(r(\mathbf{x}, \mathbf{y}))}{\int\limits_{\text{Body}} \alpha_\infty(r(\mathbf{x}, \mathbf{z}))\, d\mathbf{z}}\,, \quad \alpha_\infty(r(\mathbf{x}, \mathbf{y})) = (\langle 1 - r^4(\mathbf{x}, \mathbf{y})\rangle)^2\,. \tag{15}$$

In the isotropic case, we assume that

$$r^2(\mathbf{x}, \mathbf{y}) = \|\mathbf{x} - \mathbf{y}\|^2/(h_{\text{nl}})^2\,, \tag{16}$$

where h_{nl} is the parameter of the material that indirectly carries information about the characteristic size of the microstructure. In the case of polycrystalline metals, this parameter can be indirectly related to the average size of the grain.* In heterogeneous materials h_{nl} is a function of $\mathbf{x}$. In the nonlocal damage model for all $\mathbf{x} \in$ Body the continuity evolution law is postulated:

$$\dot{\Psi}^{\text{nl}}(\mathbf{x}) = (\dot{\Psi})^{\text{deloc}} = (-\text{PCR}\,\Psi\,\dot{\Phi}_*^{\text{local}})^{\text{deloc}}\,, \tag{17}$$

where the porosity evolution rate $\dot{\Phi}_*^{\text{local}}$ corresponds to the local damage model (11). In terms of $\dot{\Phi}$ the delocalization rule (17) takes the form

$$\dot{\Phi}_*^{\text{nl}}(\mathbf{x}) = \frac{1}{\Psi(\mathbf{x})} \int\limits_{\text{Body}} \Psi(\mathbf{y})\alpha_{\text{deloc}}(\mathbf{x}, \mathbf{y})\dot{\Phi}_*^{\text{local}}(\mathbf{y})\, d\mathbf{y} \geq 0\,. \tag{18}$$

Thus, instead of the delocalization kernel $\alpha_{\text{deloc}}(\mathbf{x}, \mathbf{y})$, the kernel proportional to $\Psi(\mathbf{y})\alpha_{\text{deloc}}(\mathbf{x}, \mathbf{y})$ is used. The desired damage trapping effect is due to the fact that heavily damaged sources $\mathbf{y}$ emanate damage only over a short distance. Finally, the following local post-processing is required to ensure the thermodynamic consistency:

$$\dot{\Phi}^{\text{local}} = \begin{cases} 0\,, & \dfrac{1}{\rho_{\text{por}}}\dfrac{1}{3\Phi}\,\mathbf{T}_{\text{ep}}^{\text{por}} : \mathbf{C}_{\text{ep}}^{\text{por}} < \dfrac{\partial\psi}{\partial\Phi}\,, \\ \dot{\Phi}_*^{\text{local}} \end{cases} \tag{19}$$

where $\dfrac{\partial\psi}{\partial\Phi} < 0$ is the partial derivative of free energy ψ with respect to porosity Φ at fixed elastic strains, $\mathbf{T}_{\text{ep}}^{\text{por}} : \mathbf{C}_{\text{ep}}^{\text{por}}$ is the trace of the stress tensor. In other words, post-processing (19) forbids the growth of porosity in the state of strong hydrostatic compression [4]. For the model under consideration, the second law of thermodynamics is satisfied, therefore this model is called thermodynamically consistent.

The Gurson–Tvergaard–Needleman model on the reference configuration. The geometrically nonlinear kinematics of the Gurson–Tvergaard–Needleman model, just as in the previous case, is based on hypotheses (1). Thus, the model uses the multiplicative decomposition of the deformation gradient tensor $\mathbf{F}$ into the elasto-plastic part $\mathbf{F}_{\text{ep}}$ and the part caused by porosity $\mathbf{F}_{\text{por}}$. In this case, the determinant $\det(\mathbf{F}_{\text{por}}) = \Phi$ has exactly the same meaning as for the thermodynamically consistent model. As a consequence, the second Piola–Kirchhoff stress tensor is calculated by a formula similar to (3):

$$\tilde{\mathbf{T}} = \frac{k}{10}\left((\sqrt{\det\mathbf{C}}/\Phi)^5 - (\sqrt{\det\mathbf{C}}/\Phi)^{-5}\mathbf{C}^{-1}\right) + \mu\mathbf{C}^{-1}(\bar{\mathbf{C}}\mathbf{C}_{\text{i}}^{-1})^D\,. \tag{20}$$

*Strictly speaking the delocalization radius h_{nl} depends on the combination of the characteristic size of the microstructure and the elasto-plastic characteristics of the material [25].

Let us note that the bulk and shear moduli are now independent of the damage accumulated in the material. The following yield function Φ_{GTN} was obtained by Gurson on the basis of the problem of deformation of a perfectly plastic medium with spherical voids:

$$\Phi_{GTN} = \frac{3}{2}\,\tilde{s}^2 - (1 + q_3 f^{*2})\sigma_m^2 + 2 f^* q_1 \cosh\left(\frac{q_2 \Phi^{-1} \mathrm{tr}\,(\mathbf{C}\tilde{\mathbf{T}})}{2\sigma_m}\right)\sigma_m^2 . \tag{21}$$

Here, q_1, q_2, and q_3 are constants, $\sigma_m = K + R$, where R is the isotropic hardening determined by the Voce law, K is the initial yield stress in a uniaxial tension test, and f^* is the modified porosity. The behavior of the material is elastic at $\Phi_{GTN} \le 0$. Viscoplastic flow starts when $\Phi_{GTN} > 0$. Along with the porosity Φ, responsible for the inelastic change in the volume, an additional porosity f determining deterioration of material strength is introduced in the Gurson–Tvergaard–Needleman model. The modified porosity $f^*(f)$, which determines the effects of accelerated coalescence of voids at the final stage of damage that precedes the formation of a macrocrack is calculated by the formula proposed by Tvergaard and Needleman:

$$f^*(f) = \begin{cases} f\,, & f \le f_c \\ f_c + K_f(f - f_c)\,, & f > f_c \\ f_u\,, & f > f_f \end{cases}, \tag{22}$$

where $K_f = \dfrac{f_u^* - f_c}{f_f - f_c}$ is the factor accelerating the growth of damage, $f_u^* = \dfrac{1}{q_1}$ is the ultimate porosity f at the moment of formation of a macrocrack, f_c is the critical porosity at the moment of acceleration of damage growth, and f_f is the value of porosity corresponding to the completely destroyed material.

The evolution equation for porosity f has the form

$$\dot{f} = A_{nucl}\sqrt{6}\lambda_i \frac{\tilde{s}}{\sigma_m^2}(1 - f)\dot{\Phi} . \tag{23}$$

Remark. In the canonical version of the Gurson–Tvergaard–Needleman model the function of the frequency of occurrence of new pores is used:

$$A_{nucl} = \frac{f_{nucl}}{s_{nucl}\sqrt{(2\pi)}} \exp\left(-0.5\left(\frac{s - \varepsilon_{nucl}}{s_{nucl}}\right)^2\right), \tag{24}$$

where f_{nucl}, s_{nucl}, and ε_{nucl} are material constants. However, for correct comparison with the thermodynamically consistent model we assume that $A_{nucl} = \mathrm{const}$.

In the classical models of plasticity, the plastic flow is assumed to be incompressible, which corresponds to conservative flow. However, in the Gurson–Tvergaard–Needleman model the yield condition depends explicitly on the hydrostatic stress component determined by Eq. (21). Thus, the normality rule (associated flow rule) leads to a nonconservative flow. In the present work, the plastic flow is divided into conservative and volumetric parts. The conservative part of the plastic flow is described by the expression

$$\frac{\mathrm{d}}{\mathrm{d}t}\mathbf{C}_i = 6\frac{\lambda_i}{\sigma_m^2}(\bar{\mathbf{C}}\mathbf{C}_i^{-1})^D\mathbf{C}_i . \tag{25}$$

The rate of change in the volume of a material particle caused by nonconservative plastic flow is calculated by the formula

$$\frac{\mathrm{d}}{\mathrm{d}t}\Phi = 3\lambda_i f^* q_1 q_2 \sinh\left(\frac{q_2\Phi^{-1}\ \mathrm{tr}\,(\mathbf{C}\tilde{\mathbf{T}})}{2\sigma_m}\right)\frac{1}{\sigma_m} . \tag{26}$$

Note that the classical conservative theory of plasticity is included as a particular case. Namely, in an undamaged material, the condition $f^* = 0$ is satisfied, which leads to incompressibility of plastic flow: $\Phi = \mathrm{const}$. The scalar intensity of plastic flow is calculated in accordance with the viscoplasticity rule:

$$\lambda_{\mathrm{i}} = \frac{1}{\eta}\left\langle \frac{f_{\mathrm{overstress}}}{f_0} \right\rangle^m , \quad f_{\mathrm{overstress}} = \mathfrak{F} - \sqrt{\frac{2}{3}}\,[K + R(s)] . \tag{27}$$

The inelastic arc length s determines the evolution of Voce-type isotropic hardening:

$$\dot{s} = \sqrt{6}\lambda_{\mathrm{i}}\,\frac{\mathfrak{F}}{\sigma_{\mathrm{m}}^2} , \quad R(s) = \frac{\gamma}{\beta}\,(1 - \exp\,(1 - \beta s)) . \tag{28}$$

Similarly to the thermodynamically consistent model, a dual variable of continuity is introduced to create the damage trapping effect. Thus, for the Gurson–Tvergaard–Needleman model we have

$$\Psi = \exp\,(-\mathrm{PCR}\,f) , \quad f = -\log\,\Psi/\mathrm{PCR} . \tag{29}$$

The rate of porosity evolution $\dot{f}^{\mathrm{local}}$ corresponds to the local damage model (23). After algebraic transformations, the delocalization rule for the Gurson–Tvergaard–Needleman model takes the form

$$\dot{f}^{\mathrm{nl}}(\mathbf{x}) = \frac{1}{\Psi(\mathbf{x})}\int\limits_{\mathrm{Body}} \Psi(\mathbf{y})\alpha_{\mathrm{deloc}}(\mathbf{x}, \mathbf{y})\dot{f}^{\mathrm{local}}(\mathbf{y})\,\mathrm{d}\mathbf{y} . \tag{30}$$

As in the case of thermodynamically consistent model, in the presented version of the Gurson–Tvergaard–Needleman model there is a damage trapping effect.

Qualitative comparison of models. The considered damage accumulation models are based on multiplicative decomposition of the deformation gradient tensor and on the application of hyperelastic constitutive relations. Both models contain the classical Simo and Miehe model [18] as a particular case. Because of this, they are w-invariant when the reference configuration is changed [4]. Despite the use of multiplicative decomposition, these models have a number of fundamental differences listed below.

1. For the thermodynamically consistent model, there is a rigorous mathematical proof of its thermodynamic compatibility [4], and this guarantees the nonnegativity of mechanical energy dissipation under any loading scenarios. At the same time, in a state of strong hydrostatic compression, the Gurson–Tvergaard–Needleman model can violate the second law of thermodynamics, which is associated with the theoretical possibility of the appearance of negative dissipation on increase in porosity under hydrostatic compression [26]. However, there are no examples of cyclic loading under which the material described by the Gurson–Tvergaard–Needleman model could turn into a perpetual motion machine of the second kind.*

2. The thermodynamically consistent model takes into account the gradual deterioration of the elastic properties of the material k and μ depending on the accumulated damage. In the Gurson–Tvergaard–Needleman model, on the contrary, the bulk and shear moduli are constant.

3. In the Gurson–Tvergaard–Needleman model, the yield condition depends on the hydrostatic component of the stress tensor, whereas in the basic version of the thermodynamically consistent model such a dependence is not provided.

4. In the thermodynamically consistent model, only one value of porosity Φ is responsible for both the change in the volume and for the damage accumulation. In the Gurson–Tvergaard–Needleman model, on the contrary, two porosity values appear: the porosity Φ responsible for the change in the volume and the porosity f that describes the damage accumulation. In this sense, the thermodynamically consistent model compares favorably with the Gurson–Tvergaard–Needleman model, since the damage measure appearing in it has a clear physical meaning.

5. In the thermodynamically consistent model, the evolution of porosity is monotonic. Thus, the effect of pore curing is excluded from consideration. In the case of high hydrostatic compression and with $f > 0$ the Gurson–Tvergaard–Needleman model, according to Eq. (26), can predict a decrease in the value of Φ. Such a decrease means partial curing (closure) of the pores. As a consequence, with a certain choice of material parameters according to Eqs. (23) and (26), a decrease in the porosity f is possible.

*It is the possibility of creating a perpetual motion machine of the second kind that is the criterion by which thermodynamically inconsistent models of the material are rejected [27].

Numerical Schemes. In the present study, a hybrid time stepping procedure for the integration of the system of evolution equations is used. We will consider in detail the implementation of a single time step for the plastic flow rule and the procedure for delocalizing the equations on the current configuration. The remaining evolution equations are integrated using the explicit Euler method.

For the thermodynamically consistent model, the plastic flow is governed by formula (5) for the material derivative of the right Cauchy–Green tensor. Based on this formula, we obtain the rule for calculating inelastic strains in the current time stepping procedure [4]:

$$ {}^{n+1}\mathbf{C}_{\mathrm{i}} = \overline{{}^{n}\mathbf{C}_{\mathrm{i}} + \frac{2\Delta t \lambda_{\mathrm{i}} \mu}{\mathfrak{F}^{\mathrm{trial}}} \left({}^{n}\Phi\right)^{-1} \overline{{}^{n+1}\mathbf{C}}} , \tag{31} $$

where $\mathfrak{F}^{\mathrm{trial}}$ is the trial driving force.

For the Gurson–Tvergaard–Needleman model, the plastic flow is assigned by formula (25). Based on the explicit solution for the implicit time-stepping procedure [28] the plastic flow is determined by the formula

$$ {}^{n+1}\mathbf{C}_{\mathrm{i}} = \overline{{}^{n}\mathbf{C}_{\mathrm{i}} + \frac{6\Delta t \lambda_{\mathrm{i}} \mu}{\sigma_{\mathrm{m}}^{2}} \overline{{}^{n+1}\mathbf{C}}} . \tag{32} $$

As in [4], the material continuity Ψ was taken as the delocalized quantity, which is dual to the porosity Φ for the thermodynamically consistent model and is dual to the porosity f for the Gurson–Tvergaard–Needleman model. The delocalization procedure is carried out on the current configuration and is the same for both models:

$$ \dot{\Psi}_{i}^{\mathrm{nl}} = \left(\sum_{j=1}^{N} \alpha_{\infty}(r(\mathbf{x}_i, \mathbf{x}_j)) \dot{\Psi}_{j}^{\mathrm{local}} V_j \det \mathbf{F}_j \right) \Bigg/ \left(\sum_{j=1}^{N} \alpha_{\infty}(r(\mathbf{x}_i, \mathbf{x}_j)) V_j \det \mathbf{F}_j \right), \tag{33} $$

where i, j are the numbers of Gauss integration points, $\mathbf{x}$ is the position vector in the current configuration, and $V_j \det(\mathbf{F}_j)$ is a scalar that specifies the volume of the element at the current time.

The averaging on the current configurations is computationally expensive as it requires a greater amount of calculations. However, as shown in [4, 29], this approach gives physically reasonable solutions. Moreover, the delocalization scheme on the current configuration ensures the objectivity and w-invariance of the resulting model [4].

Numerical Results. Let us consider the destruction of a plate made of steel of grade 20 with a hole [30]. The finite-element modeling of deformation and destruction of the plate was carried out only for its quarter with imposition of spatial symmetry conditions (Fig. 1a). In the calculations, we used four-node isoparametric finite elements with reduced stress integration and with a linear approximation of the displacements and geometry [31]. The global equations of motion are integrated using the explicit time stepping. The symmetry conditions represent mixed boundary conditions: zero displacement is prescribed for one of the components, which corresponds to the Dirichlet condition, and zero traction is specified for the other component, which corresponds to the Neumann condition. On the top end of the plate, displacements are given as time functions: $\mathrm{disp} = d_0 \left(1 - \cos\left(\frac{\pi t}{2T}\right)\right)$. The total displacement of the upper and lower ends of the plate is equal to totaldisp = 2 × disp. The plane stress is assumed in the calculations. The finite-element discretization in space is presented in Fig. 1b–d for three different finenesses. In working with nonlocal models, the delocalization kernel α_{deloc} explicitly takes into account the presence of spatial symmetries.

Model parameters were identified on the basis of an integral force–displacement curve determined in an experiment. In this case, the constants were chosen so that the calculated curve could be close to the experimental one presented in [30]. The material constants for the nonlocal thermodynamically consistent model and Gurson–Tvergaard–Needleman model are presented in Table 1.

The considered nonlocal models are reduced to local ones, if instead of the identified parameter h_{n1} a zero value is taken. The results of simulation by local approaches are presented in Fig. 2. Local relationships predict underestimated strength and crack resistance compared to the experimental data of work [30]. Structural strength here is understood as the maximum axial load leading to the formation of a macrocrack. The underestimation of the strength of the material

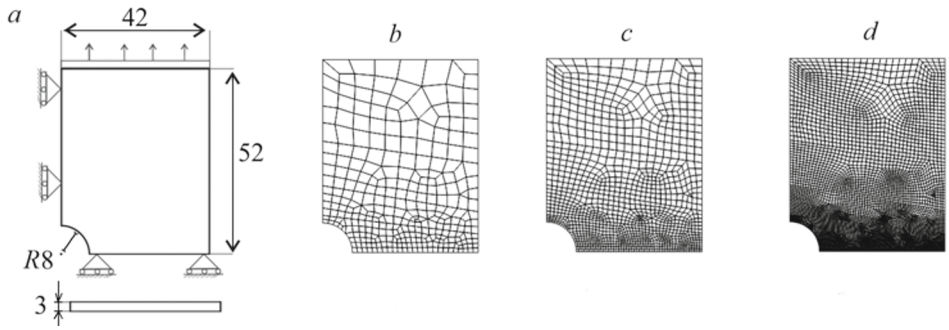

Fig. 1. Geometry of the plate with a hole (a) and its finite element discretization with 310 (b), 1240 (c), and 4960 elements (d).

TABLE 1. Constants of the TDC and GTN Models

TDC			GTN	
Elasticity parameters	k_0	175.000 MPa	k_0	175.000 MPa
	μ_0	80.760 MPa	μ_0	80.760 MPa
Plasticity parameters	K_0	280.0 MPa	K_0	280.0 MPa
	γ_0	1.850 MPa	γ_0	1.850 MPa
	β	5.05	β	5.05
Viscocity parameters	η	1.0 s	η	1.0 s
	m	1.0	m	1.0
Damage parameters	Φ_0	1.0	f_0	0.0
	A_{nucl}	0.01	A_{nucl}	0.05
	d_{growth}	1.0	q_1	1.5
	BRR	20.0	q_2	1.0
	SRR	20.0	q_3	2.25
	IRR	30.0	f_c	0.005
			f_f	0.105
Nonlocality parameters	PCR	1.0		
	h_{nl}	2.5 mm	PCR	1.0
			h_{nl}	2.5 mm

observed in the calculations in the case of inhomogeneous deformation of the structure is a well-known shortcoming of local models [3].

The distribution of the accumulated plastic strains of the material at the moment shortly after the formation of a macrocrack is shown in Fig. 3. It is noteworthy that already at the stage of subcritical deformation, the scheme of delocalization of constitutive relations significantly affects the simulation results. Thus, there is a significant difference between the fields of plastic strains obtained from local models (Fig. 3a and c) and the fields predicted by nonlocal models (Fig. 3b and d). Moreover, the difference between the local and nonlocal approaches is much larger than the difference between simulations by the Gurson–Tvergaard–Needleman and thermodynamically consistent models. This result is especially noteworthy with account for the fact that the Gurson–Tvergaard–Needleman and thermodynamically consistent models are based on a number of significantly different hypotheses.

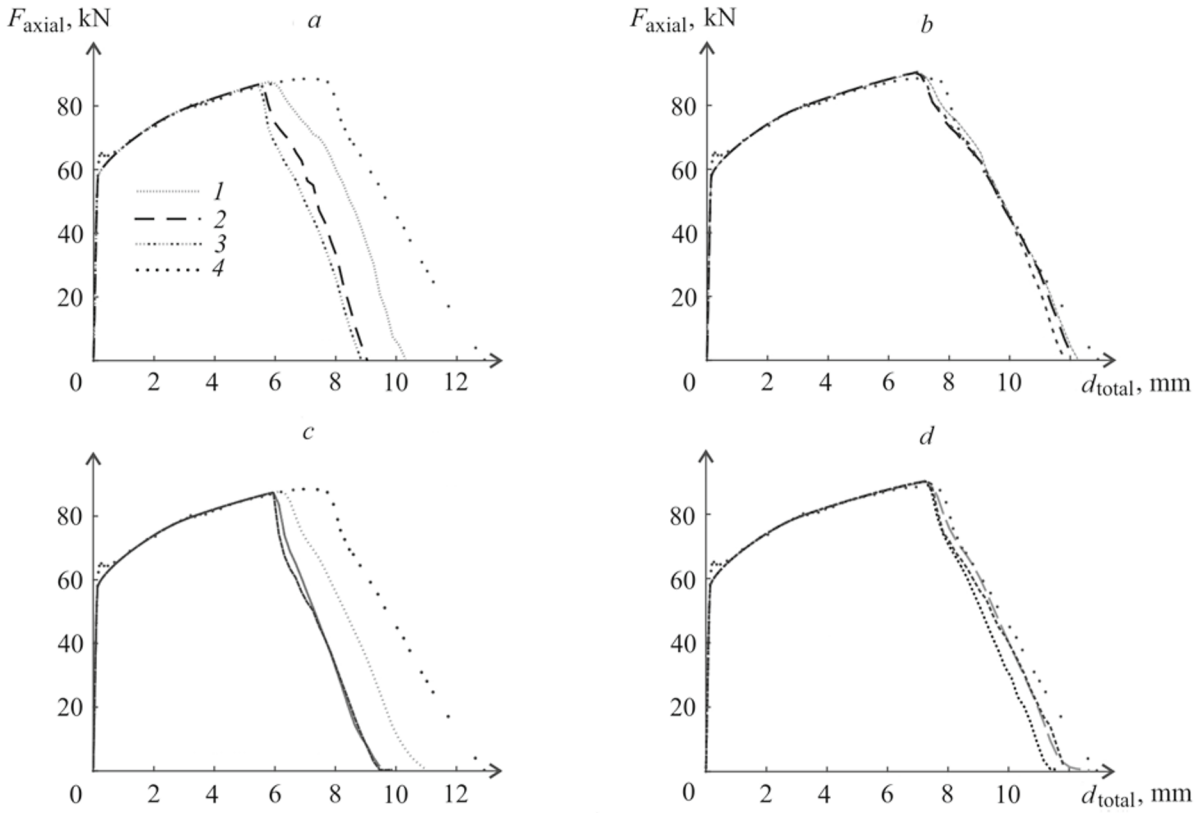

Fig. 2. Dependences of the axial force in the plate on the total displacement in it obtained with the use of local (a, c) and nonlocal (b, d) GTN (a, b) and TDC models (c, d) in the case of finite element discretization of the plate with 310 (1), 1240 (2), and 4960 elements (3); 4) experimental data [30].

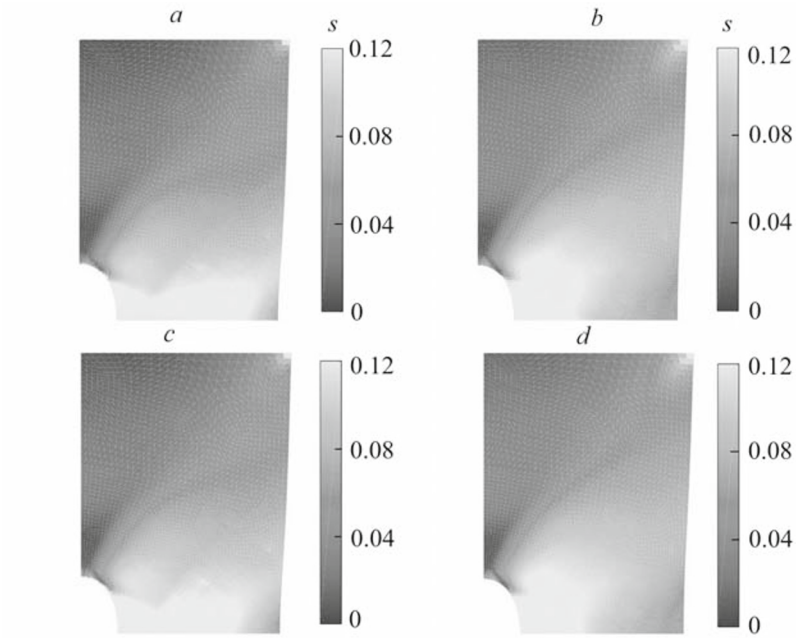

Fig. 3. Distributions of plastic strain s accumulated in the plate shortly after the initiation of a macrocrack in it (on total displacement of crack in the plate by 7.64 mm) obtained using local (a, c) and nonlocal (b, d) GTN (a, b) and TDC (c, d) models.

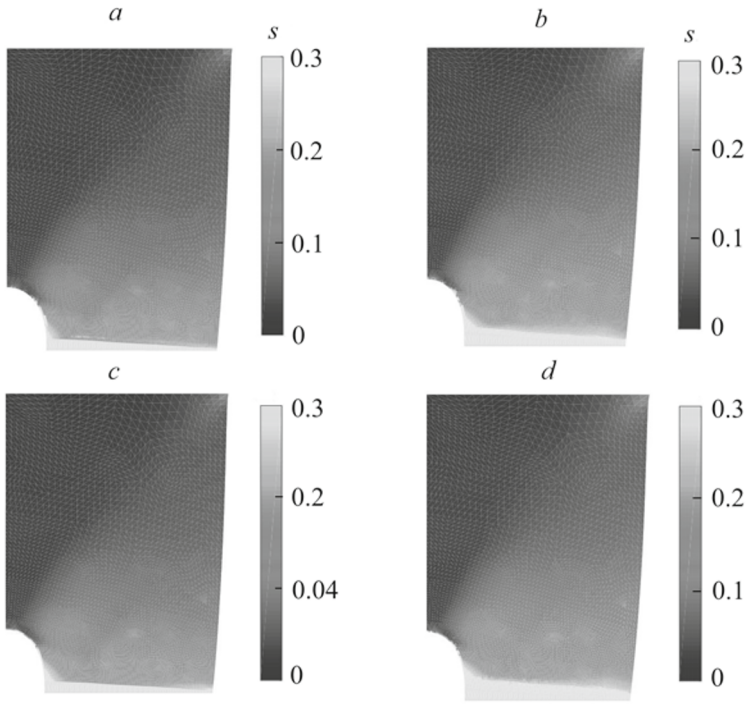

Fig. 4. Distributions of plastic strain s accumulated in the plate at the moment of its complete destruction when the axial load reaches zero, obtained using the local (a, c) and nonlocal (b, d) GTN (a, b) and TDC (c, d) models.

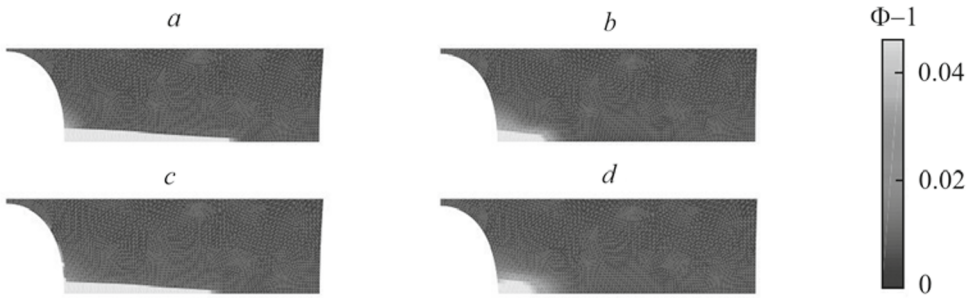

Fig. 5. Distribution of porosity Φ–1 in the plate shortly after the initiation of a macrocrack in it (on total displacement of crack in the plate by 7.64 mm) obtained using local (a, c) and nonlocal (b, d) GTN (a, b) and TDC (c, d) models. Only a part of the sample with developed damage of the material is shown.

The fields of plastic strains within samples were investigated at the stage of their complete destruction. In Fig. 4a and c one can see the localization of accumulated plastic deformations on one layer of finite elements for local simulation. In calculations using local models, a contrasting transition from the plasticized zone to the elastic one is observed, as well as relatively low energy expenditures for the initiation and propagation of a macrocrack. For the nonlocal approach, the fields of plastic strains are depicted in Fig. 4b and d. In nonlocal solutions, more energy is expended on crack initiation. Indirectly, this can be seen as a larger area of plasticization in the vicinity of the hole. In nonlocal calculations, one can also observe a smooth transition from the plasticized zone to the elastic one. As before, the difference between local and nonlocal simulation results is much larger than the difference between the Gurson–Tvergaard–Needleman and thermodynamically consistent models.

Next, we will consider the distribution of porosity in the plate for starting macrocrack. The porosity here refers to the loosening of the material Φ. The trend of similarity of nonlocal calculations by the Gurson–Tvergaard–Needleman and thermodynamically consistent models that appeared earlier is violated now (Fig. 5b and d). Thus, for the nonlocal Gurson–Tvergaard–Needleman model the porosity of the material is distributed more contrastingly along the main direction of the crack than in the calculation with the use of the nonlocal thermodynamically consistent model. This result means that the coincidence of the force–displacement curves and the fields of accumulated plastic strains does not imply the coincidence of the damage fields of the sample. In order to accurately identify the model parameters and determine the most appropriate constitutive hypotheses, additional knowledge about the local evolution of material porosity is needed.

Conclusions. A new version of the nonlocal Gurson–Tvergaard–Needleman model is proposed. Novelty compared to alternative versions [32, 33] consists in the use of a multiplicative decomposition of the deformation gradient tensor in combination with hyperplasic relations between stresses and strains, as well as in the exploitation of the damage trapping effect. Along with the new version of the Gurson–Tvergaard–Needleman model, the thermodynamically consistent model proposed in [4] is considered.

To determine the possibility of using an effective and stable computational formula (32), the equations of the Gurson–Tvergaard–Needleman model were transformed: inelastic strains were divided into a conservative (incompressible) and volumetric, and the corresponding evolution equation was proposed for each component of inelastic flow. Such a representation of the Gurson–Tvergaard–Needleman equations makes it possible to reveal the porosity parameter Φ, hidden in the conventional description, since it does not appear in the canonical equations of the Gurson–Tvergaard–Needleman model, in which the porosity f is responsible for the deterioration of strength.

The key point in this work is the conclusion about the similarity of the results of finite element calculations by two significantly different Gurson–Tvergaard–Needleman and thermodynamically consistent models. For both models, close force–displacement curves and accumulated plastic strain fields are obtained. In this case, the similarity between the Gurson–Tvergaard–Needleman and thermodynamically consistent models was observed both in the local and nonlocal approaches, which is of fundamental importance for the choice of strategies for identifying and validating these models. At the present time, the literature is dominated by methods for identifying the constants of nonlocal damage models based on integral curves [33]. Even refined methods of conducting an inhomogeneous experiment give only integral curves and strain fields [34]. However, due to the similarity of results for the Gurson–Tvergaard–Needleman and thermodynamically consistent models similar integral experimental data do not allow one to make an unambiguous conclusion in favor of one of these models.

The solution of this problem is seen by the authors in the exploitation of the property that the porosity fields Φ predicted by the Gurson–Tvergaard–Needleman and thermodynamically consistent models are significantly different. Thus, for reliable identification of parameters and validation of models, it is necessary to have detailed experimental data on the local evolution of material damage.

In the current version of nonlocal models, the integral averaging operator is based on a heuristically selected averaging kernel α_{deloc}. A more physical choice of the averaging operator is possible only if the evolution of microdefects is explicitly taken into account. Detailed information about the collective evolution of relevant microdefects can be obtained by high-resolution x-ray thermography [10–13]. Thus, the integral approach is especially promising for creating new microstructurally enriched models of damage accumulation.

Acknowledgment. The presented study was supported by a grant from the Ministry of Science and Higher Education of the Russian Federation (Project No. 075-15-2020-781).

REFERENCES

1. L. M. Kachanov, On the time of destruction under creep conditions, *Izv. Akad. Nauk SSSR*, *Otd. Tekh. Nauk*, **8**, 26–31 (1958).
2. L. Kachanov, *Introduction to Continuum Damage Mechanics*, Vol. 10, Springer Science and Business Media (1986).
3. Z. P. Bažant and M. Jirásek, Nonlocal integral formulations of plasticity and damage: Survey of progress, *J. Eng. Mech*., **128**, No. 11, 1119–1149 (2002).
4. A. V. Shutov and V. S. Klyuchantsev, Large strain integral-based nonlocal simulation of ductile damage with application to mode-I fracture, *Int. J. Plasticity*, **144**, Article ID 103061 (2021).

5. R. Vignjevic et al., SPH as a nonlocal regularization method: Solution for instabilities due to strain-softening, *Comput. Methods Appl. Mech. Eng.*, **277**, 281–304 (2014).
6. M. A. Tashkinov and A. S. Shalimov, Modeling the influence of microscale morphological parameters on the deformation behavior of porous materials with a metal matrix, *Fiz. Mezomekh*., **24**, No. 5, 130–137 (2021).
7. Z. Xue et al., Calibration procedures for a computational model of ductile fracture, *Eng. Fracture Mech*., **77**, No. 3, 492–509 (2010).
8. F. X. C. Andrade, J. M. A. César de Sá, and F. M. Andrade Pires, A ductile damage nonlocal model of integral-type at finite strains: Formulation and numerical issues, *Int. J. Damage Mech*., **20**, No. 4, 515–557 (2011).
9. V. S. Klyuchancev and A. V. Shutov, Nonlocal FEM simulations of ductile damage with regularized crack path predictions, *J. Phys.: Conf. Ser.*, **1945**, No. 1, Article ID 012018 (2021).
10. E. Maire et al., Bulk evaluation of ductile damage development using high resolution tomography and laminography, *Comptes Rendus Physique*, **13**, No. 3, 328–336 (2012).
11. C. C. Roth et al., Ductile damage mechanism under shear-dominated loading: *In-situ* tomography experiments on dual phase steel and localization analysis, *Int. J. Plasticity*, **109**, 169–192 (2018).
12. A. J. Cooper et al., A statistical assessment of ductile damage in 304L stainless steel resolved using X-ray computed tomography, *Mater. Sci. Eng.: A*, **728**, 218–230 (2018).
13. B. P. Croom et al., Collaborative ductile rupture mechanisms of high-purity copper identified by in situ X-ray computed tomography, *Acta Materialia*, **181**, 377–384 (2019).
14. A. L. Gurson, Continuum theory of ductile rupture by void nucleation and growth: Part I — Yield criteria and flow rules for porous ductile media, *J. Eng. Mater. Technol.*, **99**, No. 1, 2–15 (1977).
15. V. Tvergaard and A. Needleman, Analysis of the cup-cone fracture in a round tensile bar, *Acta Metall. Mater*., **32**, No. 1, 157–169 (1984).
16. A. V. Shutov and J. Ihlemann, Analysis of some basic approaches to finite strain elasto-plasticity in view of reference change, *Int. J. Plasticity*, **63**, 183–197 (2014).
17. A. V. Shutov, C. B. Silbermann, and J. Ihlemann, Ductile damage model for metal forming simulations including refined description of void nucleation, *Int. J. Plasticity*, **71**, 195–217 (2015).
18. J. C. Simo and C. Miehe, Associative coupled thermoplasticity at finite strains: Formulation, numerical analysis and implementation, *Comput. Methods Appl. Mech. Eng*., **98**, No. 1, 41–104 (1992).
19. H. Richter, Das isotrope Elastizitätsgesetz, *ZAMM — J. Appl. Math. Mech.*, **28**, Nos. 7–8, 205–209 (1948).
20. S. Hartmann and P. Neff, Polyconvexity of generalized polynomial-type hyperelastic strain energy functions for near-incompressibility, *Int. J. Solids Struct*., **40**, No. 11, 2767–2791 (2003).
21. A. S. Meretin and E. B. Savenkov, Mathematical model of destruction of a thermoelastic medium, *J. Eng. Phys. Thermophys*., **94**, No. 2, 365–376 (2021).
22. C. Giry, F. Dufour, and J. Mazars, Stress-based nonlocal damage model, *Int. J. Solids Struct*., **48**, Nos. 25–26, 3431–3443 (2011).
23. L. H. Poh and G. Sun, Localizing gradient damage model with decreasing interactions, *Int. J. Numer. Methods Eng*., **110**, No. 6, 503–522 (2017).
24. Z. P. Bažant and F. B. Lin, Non-local yield limit degradation, *Int. J. Numer. Methods Eng*., **26**, No. 8, 1805–1823 (1988).
25. V. N. Shlyannikov, A. V. Tumanov, and R. M. Khamidullin, The effects of gradient plasticity at the vertex of a crack under plane stress and plane strain, *Fiz. Mezomekh*., **24**, No. 2, 41–55 (2021).
26. K. Santaoja and H. Talja, Does the Gurson–Tvergaard material model satisfy the second law of thermodynamics? *J. Mech. Behav. Mater*., **11**, Nos. 1–3, 205–210 (2000).
27. C. Naumann and J. Ihlemann, On the thermodynamics of pseudo-elastic material models which reproduce the Mullins effect, *Int. J. Solids Struct*., **69**, 360–369 (2015).
28. A. V. Shutov, R. Landgraf, and J. Ihlemann, An explicit solution for implicit time stepping in multiplicative finite strain viscoelasticity, *Comput. Methods Appl. Mech. Eng*., **265**, 213–225 (2013).
29. S. Bergo, D. Morin, and O. S. Hopperstad, Numerical implementation of a non-local GTN model for explicit FE simulation of ductile damage and fracture, *Int. J. Solids Struct*., **219**, 134–150 (2021).
30. V. É. Vil′deman, E. V. Lomakin, T. V. Tret′yakova, and M. P. Tret′yakov, Supercritical deformation and failure of bodies with concentrators under plane stress conditions, *Izv. Ross. Akad. Nauk*, *Mekh. Tverd. Tela*, No. 5, 22–29 (2017).

31. P. Wriggers, *Nonlinear Finite Element Methods*, Science and Business Media, Springer (2008).
32. K. Enakoutsa, J. B. Leblond, and G. Perrin, Numerical implementation and assessment of a phenomenological nonlocal model of ductile rupture, *Comput. Methods Appl. Mech. Eng*., **196**, Nos. 13–16, 1946–1957 (2007).
33. A. Seupel, G. Hütter, and M. Kuna, On the identification and uniqueness of constitutive parameters for a non-local GTN-model, *Eng. Fracture Mech*., **229**, Article ID 106817 (2020).
34. J. P. Belnoue and A. M. Korsunsky, A damage function formulation for nonlocal coupled damage-plasticity model of ductile metal alloys, *Eur. J. Mech. A. Solids*, **34**, 63–77 (2012).